Available online at: www.basra-science-journal.org

ISSN –1817 –2695

Direct current modulation effects on the photons density in InAs/InGaAs quantum dot semiconductor laser

M.O. Oleiwi and C.A. Emshary

Physics Department , Education College for Pure Sciences, Basrah University

Basrah ,Iraq

Received 28-7-2013 , Accepted 25-9-2013

Abstract :

Different dynamics ranging from period 1 to chaos are produced in the photon density PD of InAs/InGaAs quantum dot laser QDL under the effect of injection current modulation using a theoretical model. Death phenomena in the PD of the QDL was registered too . Weak and strong modulations of the injection current led to chaotic states. Bifurcation route appears to be the main route leading to chaos .

Keywords: Quantum dot semiconductor laser , Direct current modulation, Periodic and chaotic dynamics .

Introduction

The discrete energy levels structure in semiconductor quantum dots(QDs) offers several advantages over higher –dimensional systems for the application to high-performance semiconductor laser technology ,including the potential for lower threshold current ,reduced thermal sensitivity ,and higher modulation speed [1]. QD lasers have attracted lots of attention as next –generation laser sources for fiber telecommunication networks ,because of the promising properties mentioned together with low chirp [1] .Particularly ,directly modulated lasers (DML) have been expected to play a major role in the next –generation telecommunication links for cool-less and isolator –free applications[1]. However ,one of the major drawbacks of QD lasers concerns the modulation bandwidth, which remains still limited at room temperature [2].

In principle ,direct modulation at a gigabit rate is expected to be feasible. However ,the practical rate of pulse modulation has been limited to below several hundred megahertz ,owing to the serious distortion of the output waveform caused by the relaxation oscillation of the light intensity .

The optical gain varies with the carrier density causing the number of lasing modes and the width of the spectral

envelope to increase .In order to attain practical rates of direct modulation in the gigahertz range ,it therefore appears essential to suppress relaxation oscillation in the modulated output of semiconductor lasers [3,4]. Since the main application of semiconductor lasers is a source for optical communication systems ,the problem of high-speed modulation of their output by high data rate information is one of great technological importance [5].

Aunique feature of semiconductor lasers is that, unlike other lasers that are modulated externally, the semiconductor laser can be modulated directly by modeling the excitation current .This is especially important in the view of the possibility of the monolithic integration of the laser and the modulation electronic circuit[6]. Usually it is expected that the direct modulation of semiconductor laser yields periodic pulses with a frequency (repetition rate) that is equal to the frequency of modulation [7]. For small signal sinusoidal modulation ,this is possible for a wide range of frequencies and modulation amplitudes. However, in practical situations large (strong) signal modulation is generally applied to the laser and then the nonlinear effects will come into play . Since the refractive index of the active medium of the semiconductor lasers and its cavity length depend on the semiconductor current , both the amplitude and frequency modulation of the laser radiation spectrum takes place [8].

Almost no results appeared in literature concerning the study of the effect of injection current modulation on the dynamics of quantum dot semiconductor lasers [9].In this article we present the results of the effect of injection current density modulation parameters such as bias current ,modulation current (modulation strength) and modulation frequency.

.

QD Laser Model:

The numerical investigations of the laser turn-on dynamics of the QD laser presented here are based on model given by Kathy Ludge et al [10,11] . In the QD laser system the electrons are first injected into the wetting layer WL before they are captured by the QDs. The laser dynamics is determined by the rate equations for the photon density n_{ph} of the ground state ,GS, transition ,and carrier densities in the QD , n_e and n_h and the carrier densities in the WL, w_e and w_h (e and h stand for electrons and holes, respectively) this model reads [10]:

$$\dot{n}_{ph} = -2k\,n_{ph} + \Gamma R_{ind}(n_e, n_h, n_{ph}) + \beta R_{sp}(n_e, n_h) \quad (1)$$

$$\dot{n}_e = -\frac{1}{\tau_e} n_e + S_e^{in} N^{QD} - \Gamma R_{ind}(n_e, n_h, n_{ph}) - R_{sp}(n_e, n_h) \quad (2)$$

$$\dot{n}_h = -\frac{1}{\tau_h} n_h + S_h^{in} N^{QD} - \Gamma R_{ind}(n_e, n_h, n_{ph}) - R_{sp}(n_e, n_h) \quad (3)$$

$$\dot{w}_e = \eta \frac{j(t)}{e_o} + \frac{n_e}{\tau_e} \frac{N^{sum}}{N^{QD}} - S_e^{in} N^{sum} - \tilde{R}_{sp}(w_e, w_h) \quad (4)$$

$$\dot{w}_h = \eta \frac{j(t)}{e_o} + \frac{n_h}{\tau_h} \frac{N^{sum}}{N^{QD}} - S_h^{in} N^{sum} - \tilde{R}_{sp}(w_e, w_h) \quad (5)$$

$R_{ind}(n_e, n_h, n_{ph}) = WA(n_e + n_h - N^{QD})n_{ph}$ is the linear gain, N^{QD} denotes twice the QD density of the lasing subgroup (the factor of 2 accounts for spin degeneracy), W is the Einstein coefficient, and A is the WL normalization area ($A = 4\mu m \times 1mm$).

The density N^{sum} is twice the total QD density . The spontaneous emission in the QDs is approximated by $R_{sp}(n_e, n_h) = (W / N^{QD})\, n_e\, n_h$.
$\tilde{R}_{sp}(w_e, w_h) = B^S\, w_e\, w_h$ expresses the WL spontaneous recombination rate where B^S is the band–band recombination coefficient in the WL. β is the spontaneous emission coefficient and $\Gamma = \Gamma_g\, N^{QD} / N^{sum}$ is the optical confinement factor. Γ is the product of the geometric confinement factor Γ_g (i.e the ratio of the volume of all QDs and the mode volume) and the ratio N^{QD} / N^{sum} . The total cavity loss is expressed by $2k$. The variable $j(t)$ is the injection current density, e_o is the electronic charge, and $\eta = 1 - w_e / N^{WL}$ is the injection efficiency that accounts for the fact that we cannot inject any more carriers if the WL is already filled $(w_e = N^{WL})$. A sketch of the epitaxial structure as well as the energy diagram of the band structure is shown in Fig. (1) [10].

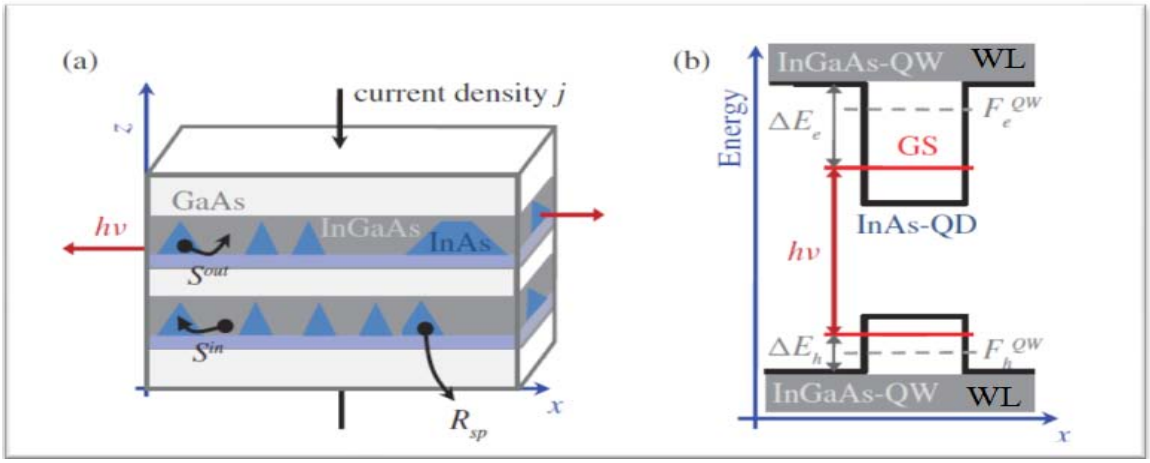

Fig. 1. (a) Schematic illustration of the QD laser. (b) Energy diagram of the band structure across a QD. *hv* labels the ground state (GS) lasing energy. ΔE_e and ΔE_h mark the distance of the GS from the (quantum well) QW band edge for electrons and holes, respectively. F_e^{QW} and F_h^{QW} are the quasi-Fermi levels for electrons and holes in the QW, respectively [10].

The spectral properties of the laser output are not addressed in the model, as the photon density is an average over all longitudinal modes. Changes in the QD size distribution are taken into account only by changes in the active QD density, which basically changes the gain. The values of parameters used in our simulations are listed in Table 1. A crucial contribution to the dynamics of QD lasers is given by the nonradiative carrier–carrier scattering rates (nonlinear scattering rates) S_e^{in} and S_h^{in} for electron and hole capture into the QD levels, S_e^{out} and S_h^{out} for carrier escape from the QD levels, and scattering times $\tau_e = (S_e^{in} + S_e^{out})^{-1}$ and $\tau_h = (S_h^{in} + S_h^{out})^{-1}$ [2]. These rates are determined microscopically within the Boltzmann equation and orthogonalized plane-wave approach . All electron–electron, hole–hole, and mixed electron–hole Auger processes are included

in the rates . When WL carrier density is very high, the capture dynamics within the QD-WL structure is dominated by Coulomb scattering (nonlocal Auger recombination).The calculated scattering rates depend in a strongly nonlinear way upon the WL carrier densities . The rate equations (1-5) predict stable behavior ,so we needs to add at least one additional degree of freedom to allow the occurrence output non periodicity and chaos .There are several possibilities to accomplish this [12]. The easiest one is to modulate the injection current periodically with a modulation frequency ω_m .The injection current density in the pumping term [$\eta \frac{j(t)}{e_0}$] equations (4) and (5) has to be replaced by a source of injection current like [7] :

$$j(t) = j_b + j_m \sin(2\pi f_m t) \text{ .....(6)}$$

Where j_b is the dc part of the injection current and j_m is the amplitude of the ac part of the injection current .

$j_b = b \times j_{th}$, b is the bias strength,

$j_m = m \times j_{th}$, m is the modulation depth

f_m $(= \frac{\omega_m}{2\pi})$, is the modulation frequency.

j_{th} : is threshold current density ($j_{th} = 90.5\, A cm^{-2}$ [13]).

Results and discussion :

The rate equations (1-5) are solved numerically using the fourth –order Runge–Kutta method
with step time size is (0.1 ns) and Mat lab system .The parameter values used in the simulations are given in table (1) [10]. S_e^{in} , S_h^{in} , S_e^{out} and S_h^{out} are calculated using separate relations [13] .

Table (1) parameter values used for numerical simulation

Symbol	Meaning of symbol	Value
W	The Einstein coefficient	$0.7\,ns^{-1}$
T	Temperature	300 K
2κ	The total cavity loss	$0.1\,ps^{-1}$
Γ_g	The geometric confinement factor	0.075
Γ	Optical confinement factor	2.25×10^{-3}
ΔE_e	Energy difference between GS level of QD and WL (electrons)	$190meV$
A	WL normalization area	$4\times10^{-5}\,cm^2$
N^{QD}	Twice the QD density of the lasing subgroup	$0.6\times10^{10}cm^{-2}$
N^{sum}	Twice the total QD density	$20\times10^{10}cm^{-2}$
N^{WL}	Carriers density in WL	$2\times10^{13}cm^{-2}$
B^S	The band–band recombination coefficient in the WL	$850ns^{-1}\,nm^2$
β	The spontaneous emission coefficient	5×10^{-6}
$m_e\,(m_h)$	The effective mass of electron (hole)	$0.043\,(0.45)\,m_0$
ΔE_h	Energy difference between GS level of QD and WL (holes)	69 meV

The injection parameters i.e the dc bias current, j_b , the dc bias strength ,*b*, the modulation current , j_m , modulation depth ,m, and modulation frequency, f_m , have been chosen according to Table (2).

Table (2) Injection parameters

Symbol	Meaning of symbol	Value									
b	the dc bias strength	1			1.3			1.8		2.5	
m	modulation depth	0.1	0.4	0.5	1	1.3	1.5	2	5	9	14
$f_m\,(GHz)$	modulation frequency	0.1	0.3	0.5	0.8	1	2	3	4	5	10

For small values of modulation strength (*m*=0.1) ,(*b*=1) and modulation frequency less than 3GHz the laser operates in the period 1 at $f_m = 0.1GHz$ then it switched to period 4 state at $f_m = 1GHz$ up to $f_m = 2\ GHz$ .Mixed state which consist of chaos followed by period 4 then period 3 states $f_m = 3GHz$ appeared .At $f_m = 4GHz$ severe chaotic state appears. When inspected deeply developed chaos can be noticed. Such state sustained along the signal which lasted up to 400ns .For $f_m \rangle 4GHz$ special signal appeared ,short lived chaotic state followed by distorted period 1 or period 2. Keeping *b=1* and varying m through 0.4 ,0.6 ,0.8,1,and $f_m = 0.1GHz$,pulsating output appears a 6ns train of pulses of the same shape that dies for a period of *t=4ns* and so on (fig.2),

such behavior is called death usually seen

to occur in semiconductor lasers either under the effect of feedback [12,15] or under the synchronization with another semiconductor lasers [16]. For higher value of the dc part of injection current i.e *b=1.3* and *m=0.1* then increasing the modulation frequency in the range *(0.1-5) GHz* we have noticed the following :sustained period 1 appeared up to $f_m = 2GHz$ then periodic chaos state appeared at $f_m = 3GHz$ up to 5GHz (fig 3).When $f_m = 4GHz$ two types of dynamics can be seen ,a chaotic signal followed by deformed period 1. Raising *m* to 0.5 keeping *b=1.3* and varying f_m through the same mentioned range have noticed the following : periods 1 and 2 overcome the dynamics of different shapes except the case $f_m = 5GHz$ when chaotic signal appeared as can be seen in (fig. 4) .Death phenomena occurs too. When m=1 and $f_m = (0.1-5)\ GHz$ period 1 sustained with the occurrence of death phenomena once again . At *m=1.3* and *b=1.3* and f_m *=(0.1-5)GHz* more dynamics are of period 1 with the death phenomena to occur more frequent (fig 5). When *m=1.5,b=1.3* and $f_m = (0.1-5)\ GHz$ the following is noticed :up to $f_m = 3GHz$ mainly period 1 appeared together with a series of pulses separated by death regions .At $f_m = 4GHz$ mixture of period 1, period 2 and period 3appeares as can be seen in (fig .6) which switches to an intermittency state where long series of period 1 state separated by odd signal or double signals when f_m =5*GHz* (fig 7). By fixing *b=1.8* and varying *m* between (0.1-5) and f_m vary between $(0.1-5)\ GHz$. The following are noticed :when $f_m = 0.8\ GHz$ and *m=0.1* period 1 state occurs while at $f_m = 1\ GHz$ chaotic output followed by period 1 once more as f_m increased. At $f_m = 4\ GHz$ severe chaos seen to occur through to $f_m = 5\ GHz$ as shown in fig (8) .Increasing *m to 0.5* with *b=1.8* leads to period 1 state .The combination of period 1 and death region separated signals appeared when *m=1,1.5* and 2 ,while period 2 followed by period 1 then chaos occurs when *m=5* and f_m ranged between 1 and *3 GHz* as shown in fig (9), period 1 retained when f_m *= 4 and 5 GHz.* Increasing *b* to *2.5* then varying *m* between *0.1 and 5* $f_m = (0.1-5)\ GHz$ we have noticed the following : For m=0.1 period 1 state appears first up to $f_m = 0.5\ GHz$ which switches to chaotic state for $f_m = (0.8-1)\ GHz$. At $f_m = 2\ GHz$ the period 1 state recovered once more then period 2 at f_m *=3G GHz and 4GHz* then the systems enters a severe chaotic state (see fig 10). Raising m to 0.5 we see the followings: Period 1 appeared up to $f_m = 3\ GHz$ then chaos occurs for $f_m = 4\ GHz$ and above . For *m=1.3* and f_m increased up to 3GHz periods 1and 2 appeared which breaks to chaos at $f_m \geq 4\ GHz$ (see fig.11). As *m=2* the system run-through period 1 state to period 2 state then period 1 once more as can be seen in fig 12 . The same behavior seen for *m=5.* For *m=9* , fig (13) shows the sort of output that appears when f_m varied between *2GHz to 5GHz* a sustained period 1 followed by period 2 occurs then period 1 again. Increasing *m* further to 14 we noticed the results shown in fig (14) with special case when $f_m = 10\ GHz$ (fig (15)),where chaos results.

Increasing the current density increases on the population inversion and relaxation frequency [17] , and also affects on the gain of the device , i.e. it has effects on the refractive index and line-width

enhancement factor .Relaxation frequency depends on life time of photons and pumping flux and both are proportional to current density and the spontaneous emissions rate. Obtained results agree with those of other researchers concerning other types of lasers such as multiple quantum wells [4],lasers under feedback [18] and bi-directionally coupled semiconductor lasers[19]. Instabilities and chaotic phenomena in class B lasers (semiconductor lasers are candidate for such class) critically depend both on the spontaneous emission and the gain saturation [6].
When a semiconductor laser is modulated at a frequency above the intrinsic resonance frequency ,the resonance peak shifts lower frequency as the modulation current increased .When the frequency of the noise peak is moved to about half of the drive frequency ,the noise peak begins to the sharpened .That is the first harmonic is about to be generated .When the modulation current is increased further, the oscillation gradually becomes period – 1, and so on. They combination (j_b, j_m, f_m) need not to be chosen to insure low or strong modulation as the obtained results proved that instabilities can be achieved for low biased current and m but high frequency of modulation .Table (3) tabulated the ranges of (b, m , f_m) or (j_b, j_m, f_m) that leads to instabilities of chaos in the output of QDLs.

Table (3) :Chaotic conditions

b ($j_b(Acm^{-2})$)	m ($j_m(Acm^{-2})$)	$f_m\,(GHz)$
1 (90.5)	0.1 (9.05)	4
1.3 (117.6)	0.1 (9.05)	3
1.3 (117.6)	0.1 (9.05)	4
1.3 (117.6)	0.1 (9.05)	5
1.3 (117.6)	0.5 (45.2)	5
1.3 (117.6)	1.5 (135.7)	5
1.8 (162.9)	0.1 (9.05)	1
1.8 (162.9)	0.1 (9.05)	4
1.8 (162.9)	0.1 (9.05)	5
1.8 (162.9)	1 (90.5)	5
1.8 (162.9)	5 (452.5)	3
2.5 (226.2)	0.1 (9.05)	1
2.5 (226.2)	0.1 (9.05)	5
2.5 (226.2)	1.3 (117.6)	5
2.5 (226.2)	14 (1267)	10

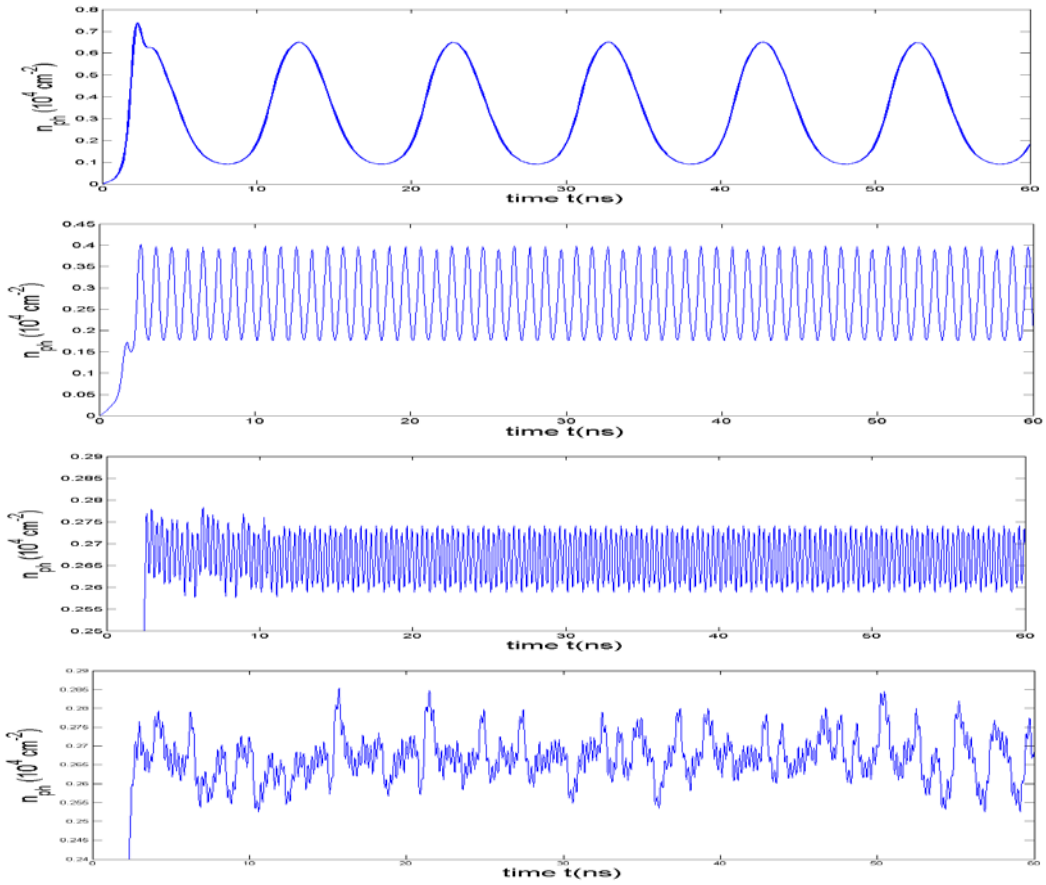

Fig (2a):Time series of photon density (n_{ph}) for selected bias strength, *b* ,modulation depth ,*m*,and modulation frequency (GHz) , f_m ,(b,m, f_m): (i) 1, 0.1, 0.1 ; (ii) 1, 0.1, 1 ; (iii) 1, 0.1, 3 ; (iv) 1, 0.1, 4.

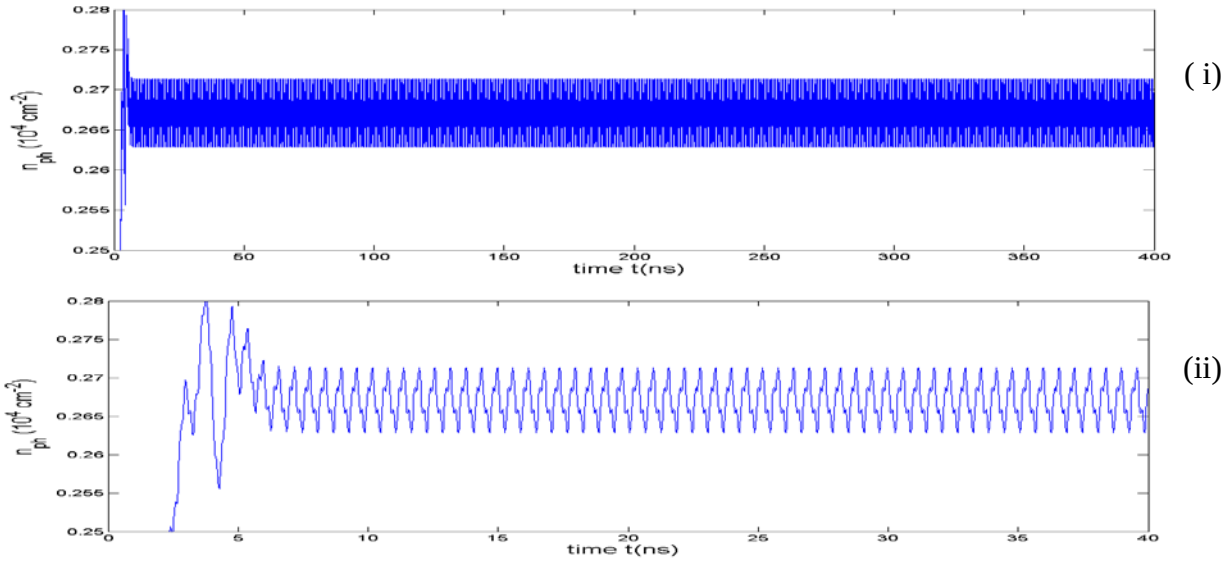

Fig (2b):Time series of photon density (n_{ph}) for selected bias strength, *b*, modulation depth ,*m*, and modulation frequency (GHz) , f_m ,(b,m, f_m): 1, 0.1, 5 for two time bases : i (0-400 ns), ii(0-40ns)

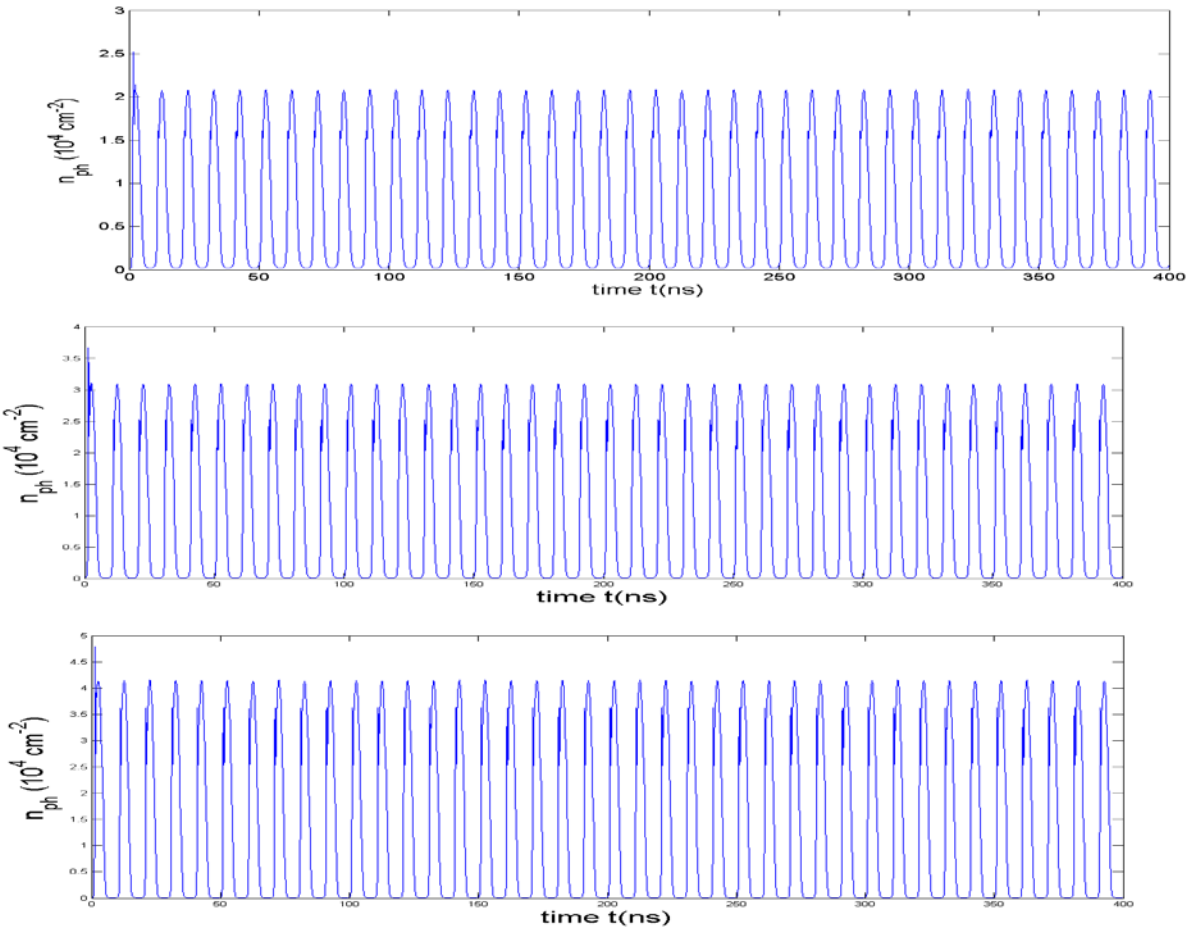

(i)

(ii)

(iii)

Fig (2c):Time series of photon density (n_{ph}) for selected bias strength, *b*, modulation depth ,*m*, and modulation frequency (GHz) , f_m ,(b,m, f_m): (i) 1,0.4,0.1 ; (ii) 1,0.6 ,0.1 ;(iii) 1,0.8,0.1.

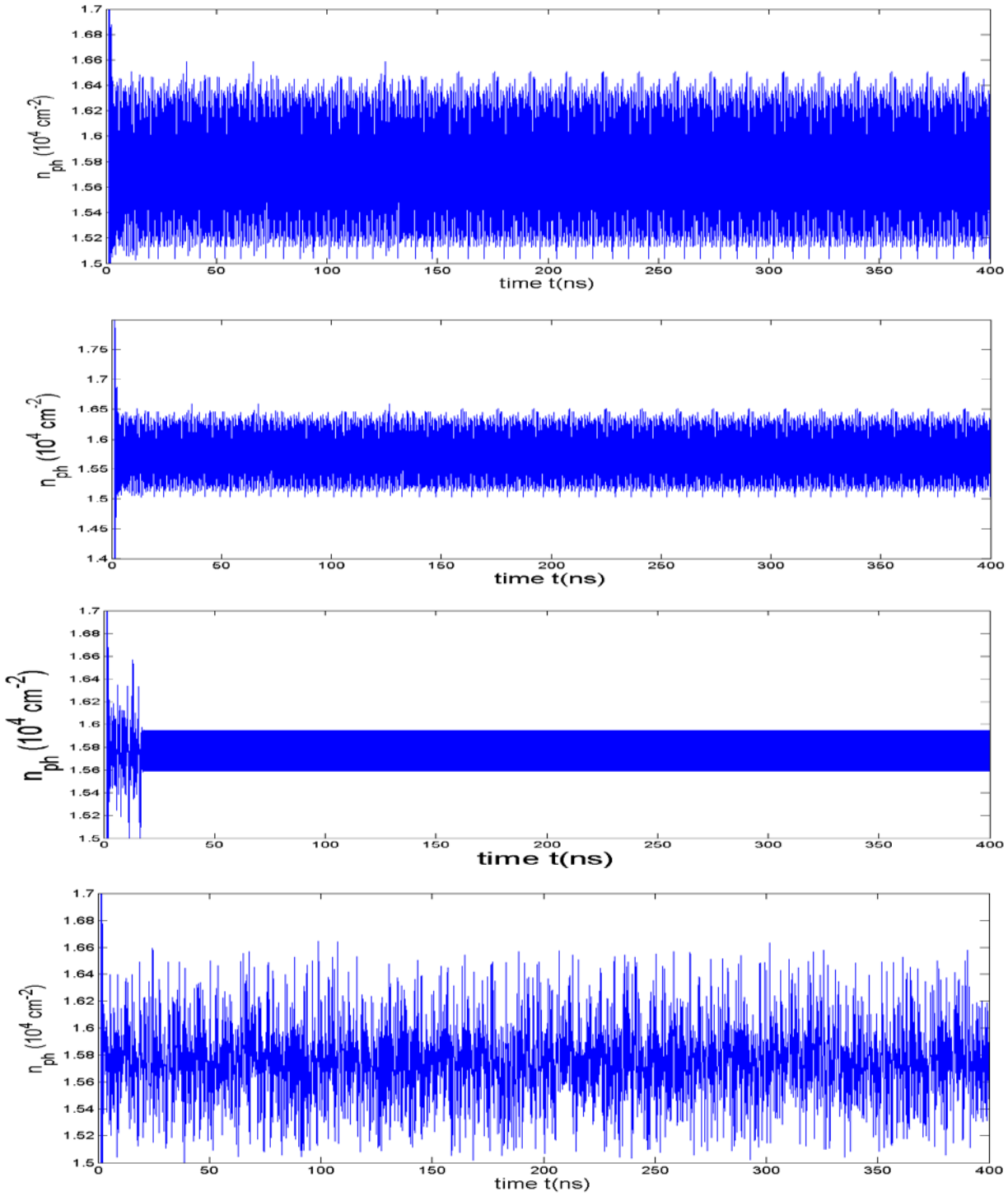

Fig (3):Time series of photon density (n_{ph}) for selected bias strength, *b*, modulation depth ,*m*, and modulation frequency (GHz) , f_m ,(b,m, f_m) : (i) 1.3, 0.1, 2 ; (ii) 1.3, 0.1, 3 ;(iii) 1.3, 0.1, 4; (iv) 1.3,0.1,5.

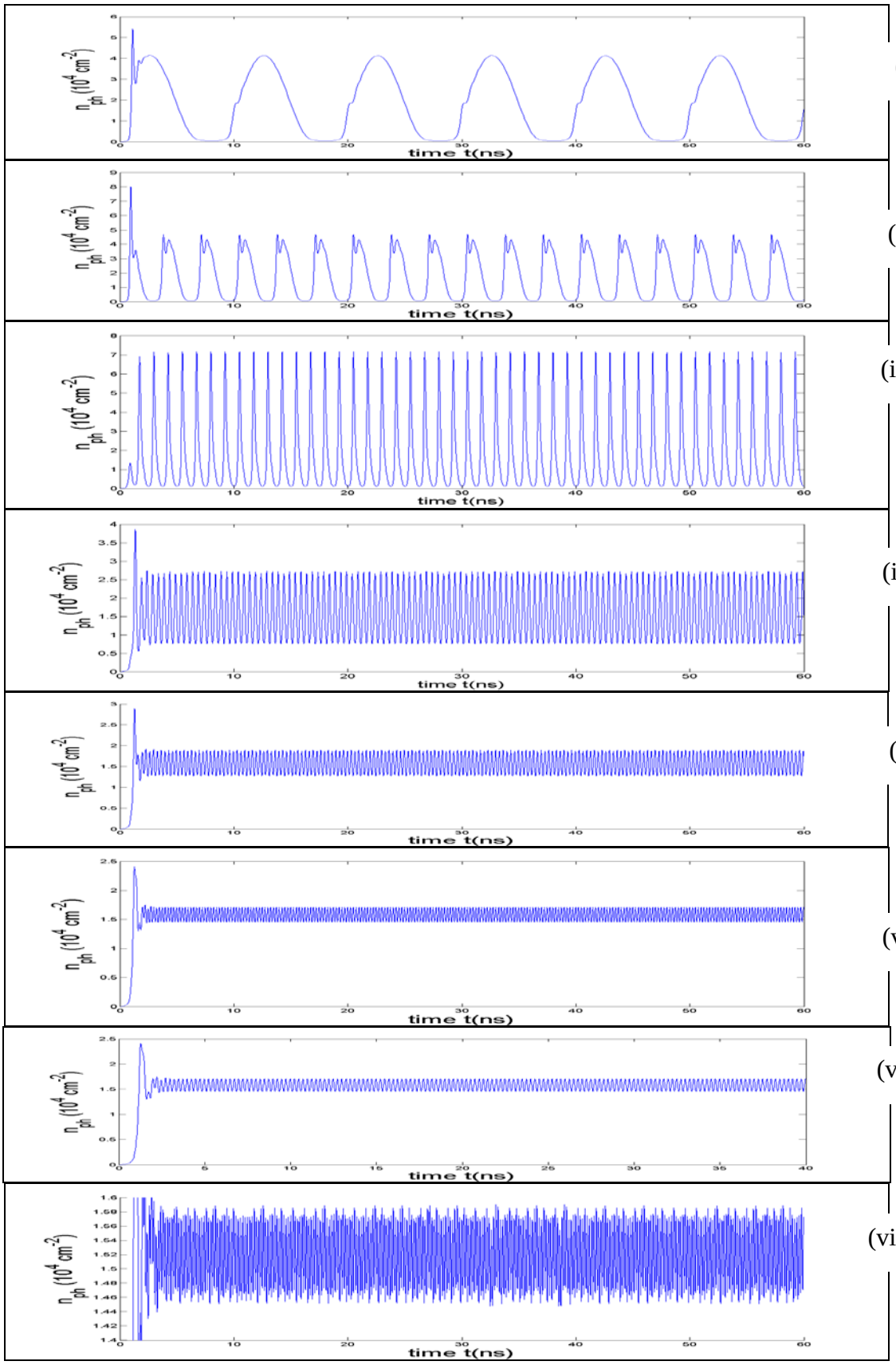

Fig (4):Time series of photon density (n_{ph}) for selected bias strength, *b*, modulation depth ,*m*, and modulation frequency (GHz) , f_m ,(b,m, f_m): (i) 1.3, 0.5, 0.1 ; (ii) 1.3, 0.5, 0.3 ;(iii) 1.3, 0.5,0.5;(iv)1.3,0.5,0.8;(v)1.3,0.5,2;(vi) 1.3,0.5,3 ; (vii) 1.3, 0.5, 4 ;(viii) 1.3,0.5,5.

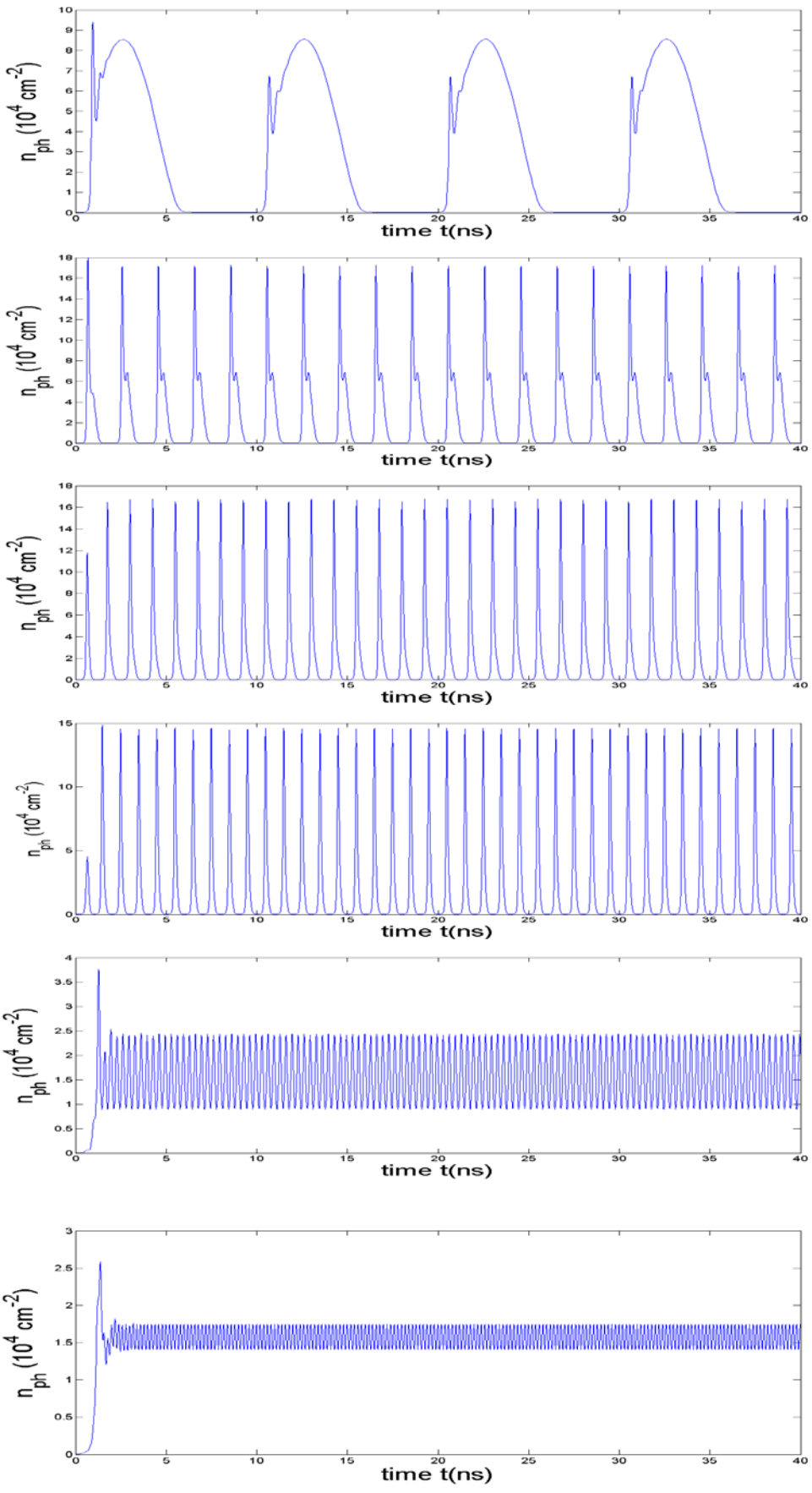

Fig (5):Time series of photon density (n_{ph}) for selected bias strength, *b*, modulation depth ,*m*, and modulation frequency (GHz) , f_m ,(b,m, f_m): (i) 1.3, 1.3, 0.1 ; (ii) 1.3, 1.3, 0.5 ;(iii) 1.3, 1.3,0.8;(iv)1.3,1.3,1;(v)1.3,1.3,3; (vi) 1.3, 1.3, 5.

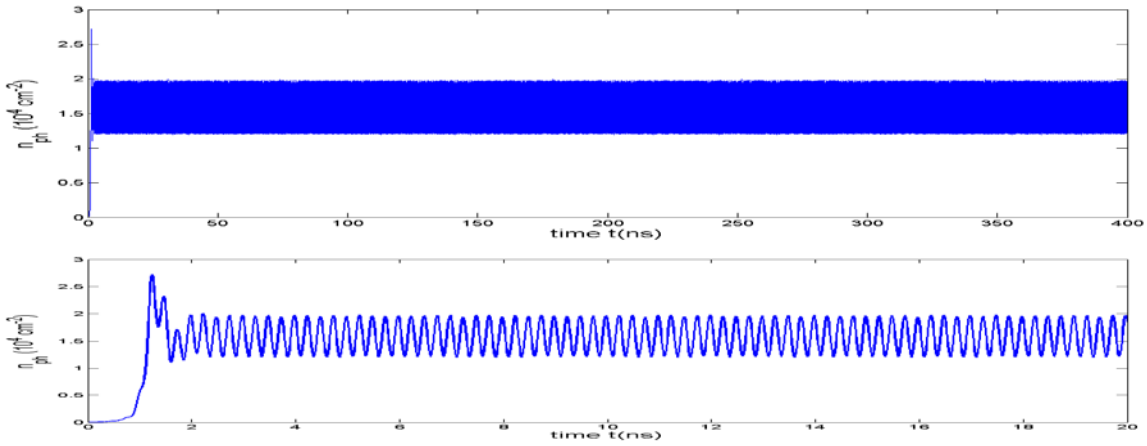

(i)

(ii)

Fig (6):Time series of photon density (n_{ph}) for selected bias strength, *b*, modulation depth ,*m*, and modulation frequency (GHz) , f_m ,(b,m, f_m): 1.3, 1.5, 4 for two time bases :i(0-400 ns),ii(0-20 ns)

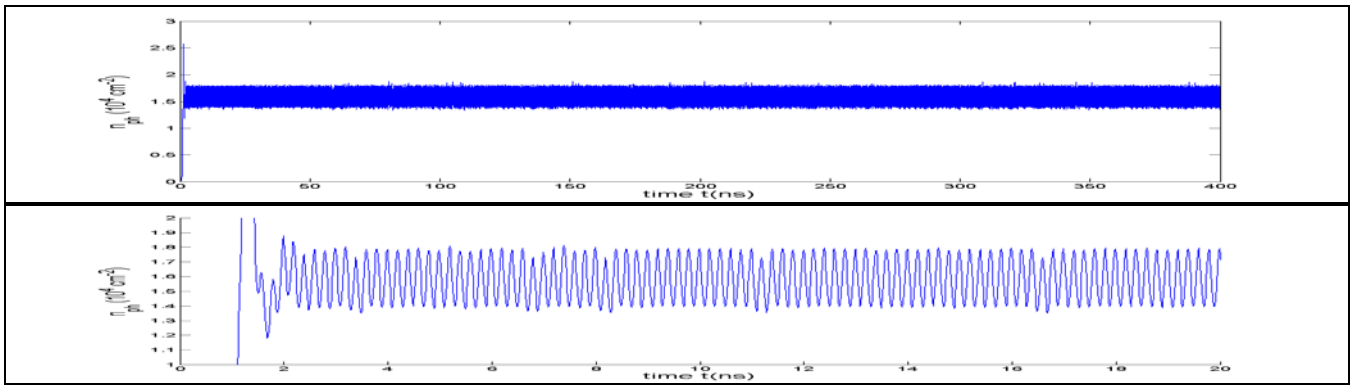

(i)

(ii)

Fig (7):Time series of photon density (n_{ph}) for selected bias strength, *b*, modulation depth ,*m*, and modulation frequency (GHz) , f_m ,(b,m, f_m): 1.3, 1.5, 5 for two time bases :i(0-400 ns),ii(0-20 ns)

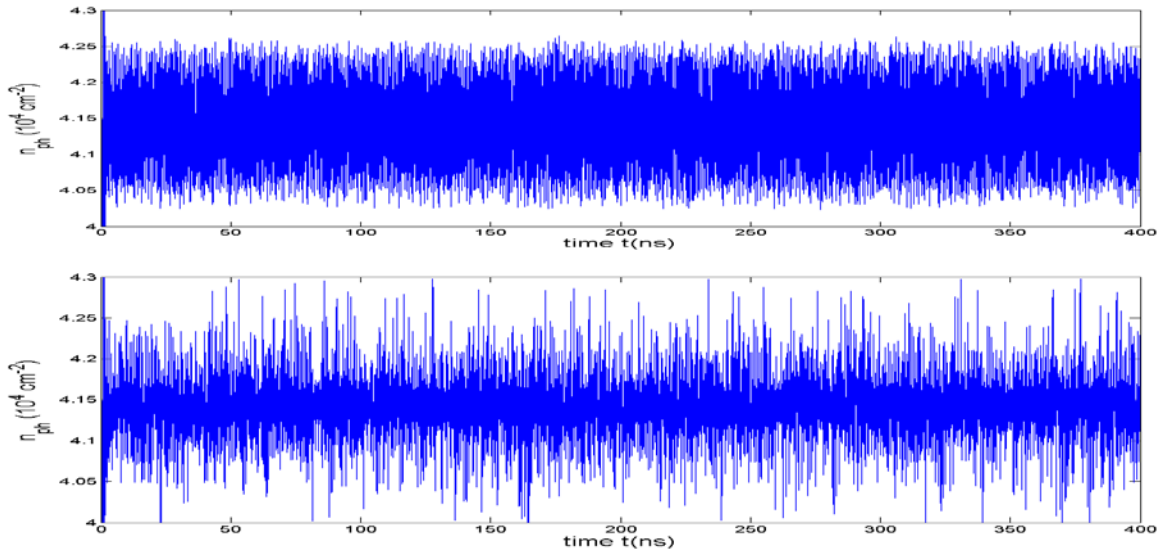

(i)

(ii)

Fig (8):Time series of photon density (n_{ph}) for selected bias strength, *b*, modulation depth ,*m*, and modulation frequency (GHz) , f_m ,(b,m, f_m): (i) 1.8, 0.1, 4 ; (ii) 1.8, 0.1,5 .

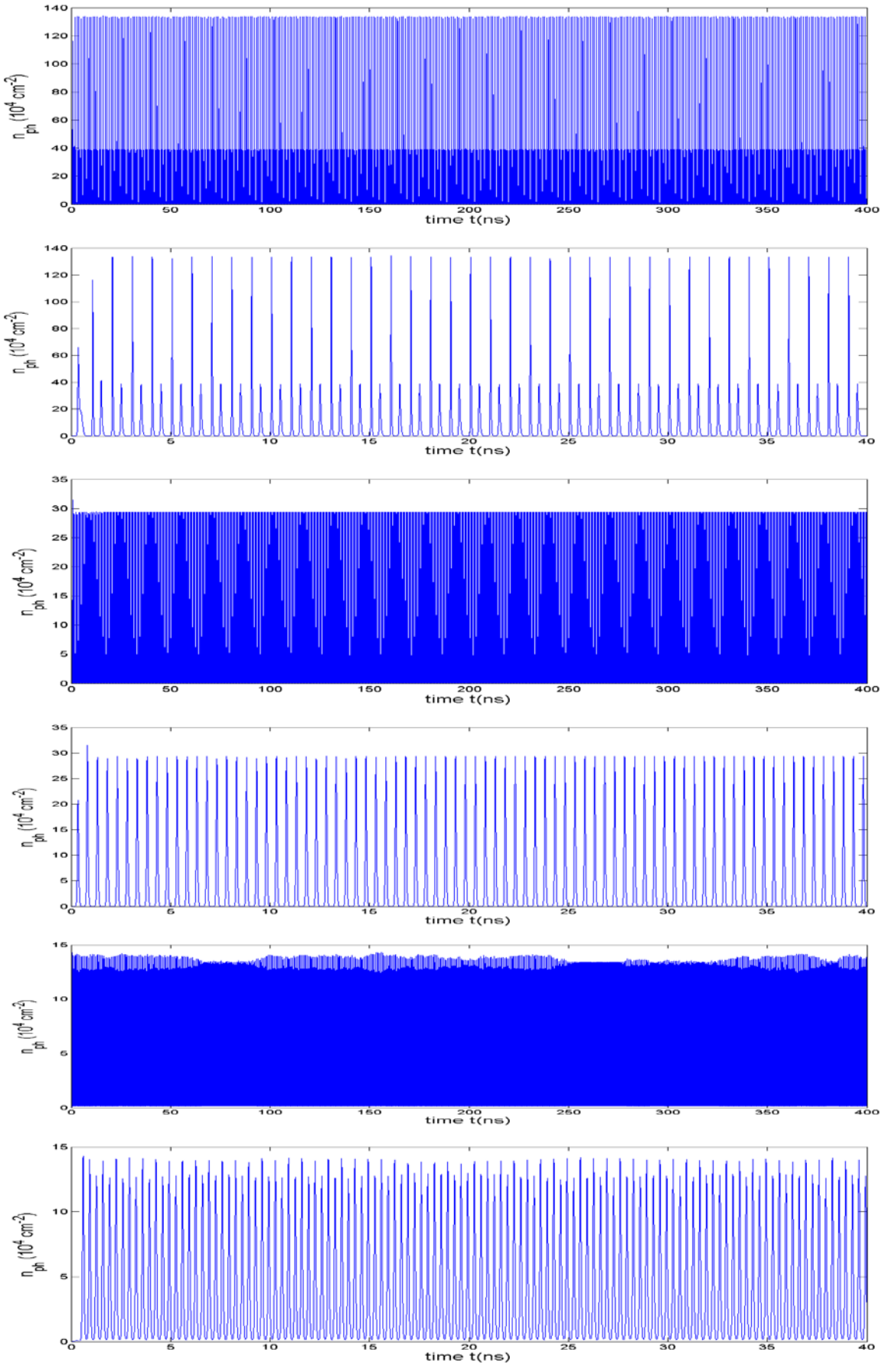

Fig (9):Time series of photon density (n_{ph}) for selected bias strength, *b*, modulation depth ,*m*, and modulation frequency , f_m , : (i) 1.8, 5, 1 ; (ii) 1.8, 5, 1 ;(iii) 1.8, 5, 2 ; (iv)1.8, 5, 2; (v)1.8, 5,3 ; (vi) 1.3,0.5,3 .

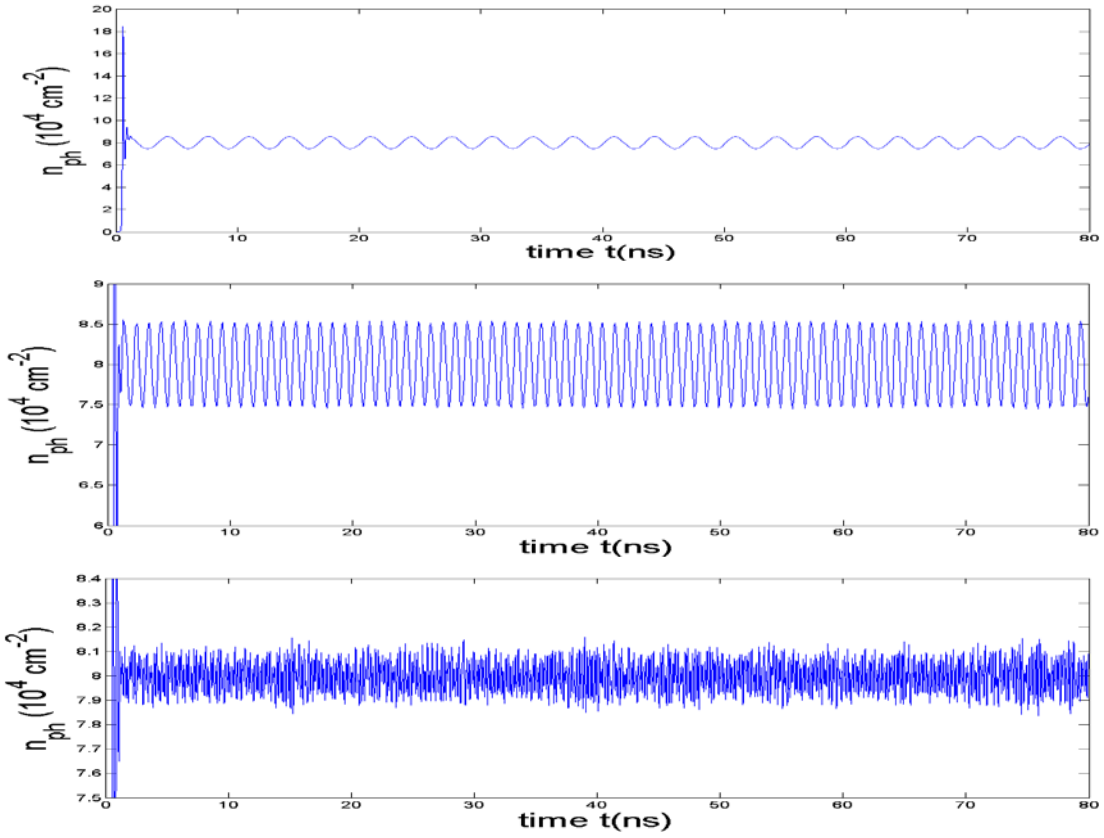

(i)

(ii)

(iii)

Fig (10):Time series of photon density (n_{ph}) for selected bias strength, *b*, modulation depth ,*m*, and modulation frequency (GHz) , f_m ,(b,m, f_m): (i) 2.5, 0.1, 0.3 ; (ii) 2.5, 0.1, 1 ; (iii) 2.5,0.1,5 .

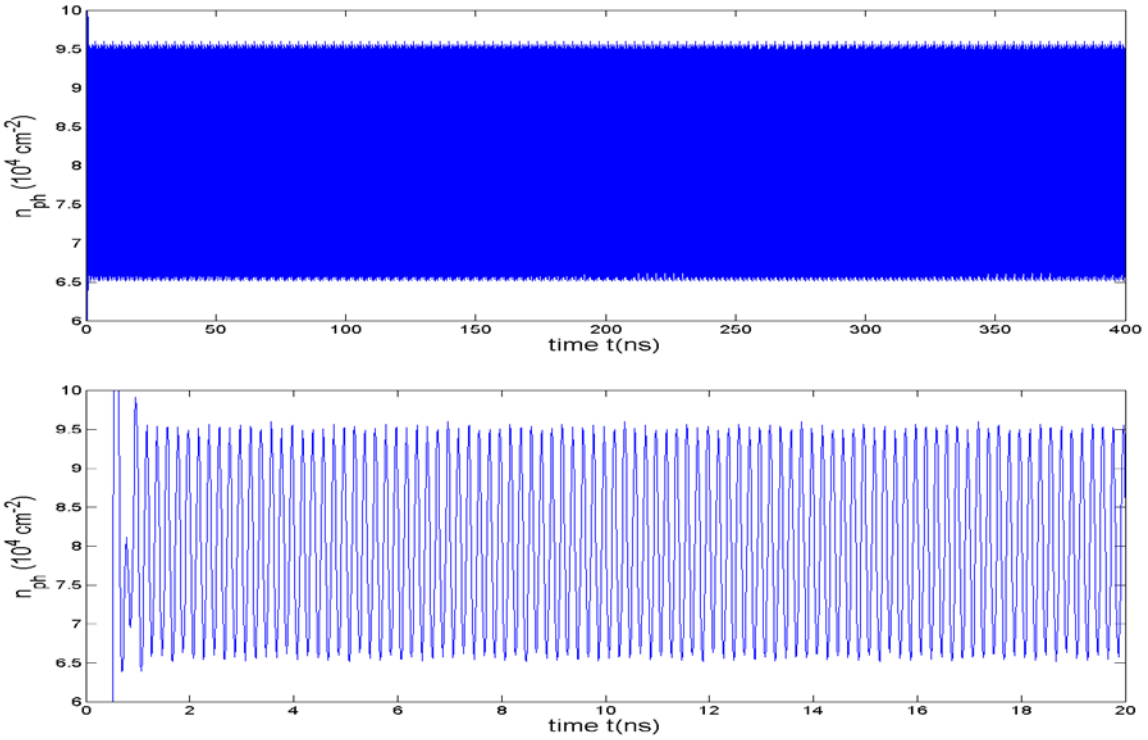

(i)

(ii)

Fig (11):Time series of photon density (n_{ph}) for selected bias strength, *b*, modulation depth ,*m*, and modulation frequency (GHz) , f_m ,(b,m, f_m): 2.5, 1.3, 5 for two time bases : i(0-400 ns),ii(0-20 ns)

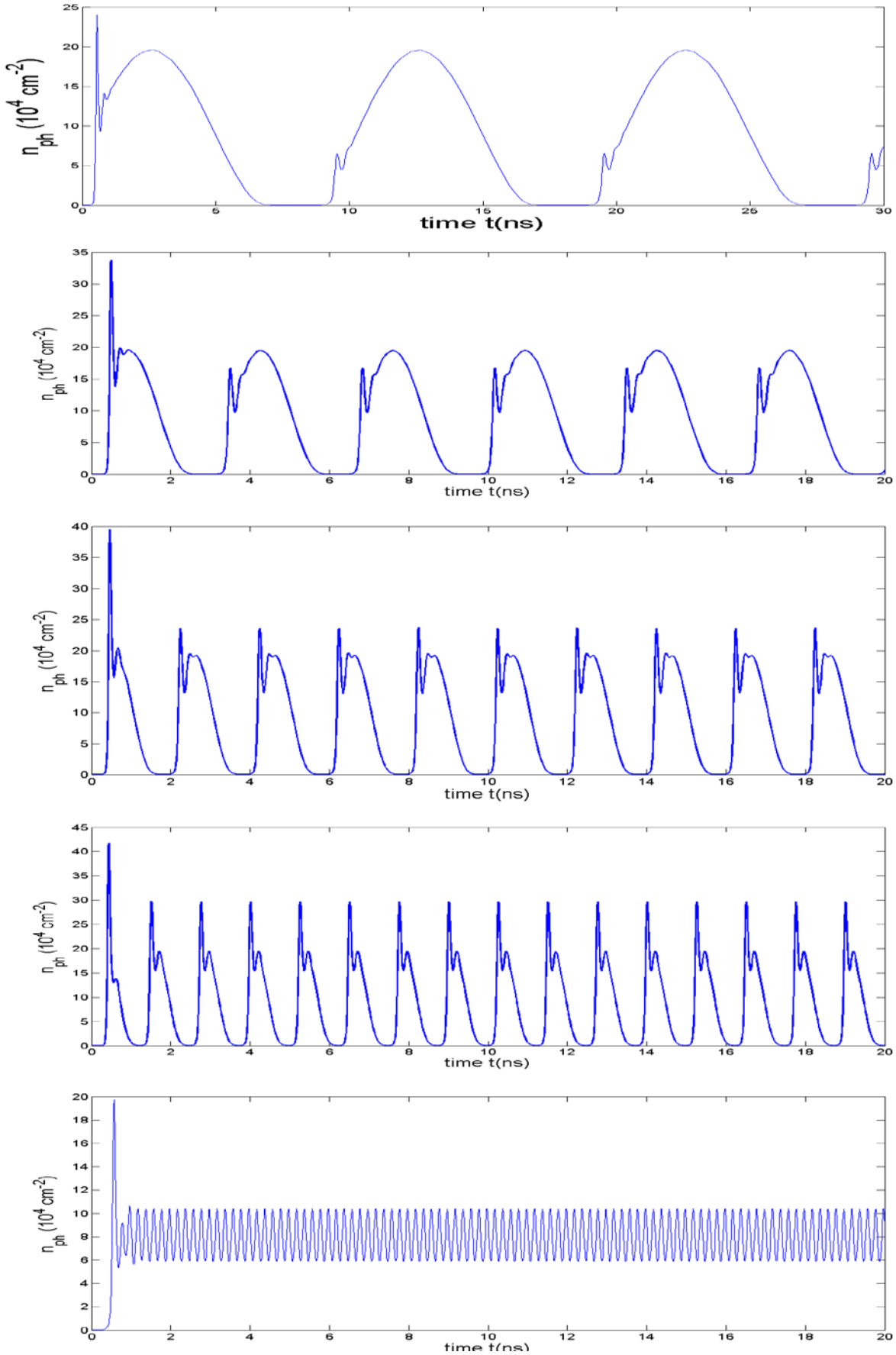

(i)

(ii)

(iii)

(iv)

(v)

Fig (12):Time series of photon density (n_{ph}) for selected bias strength, *b*, modulation depth ,*m*, and modulation frequency , f_m , : (i) 2.5, 2 , 0.1 ; (ii) 2.5, 2, 0.3 ;(iii) 2.5, 2 , 0.5; (iv) 2.5, 2 , 0.8;(v) 2.5,2,5.

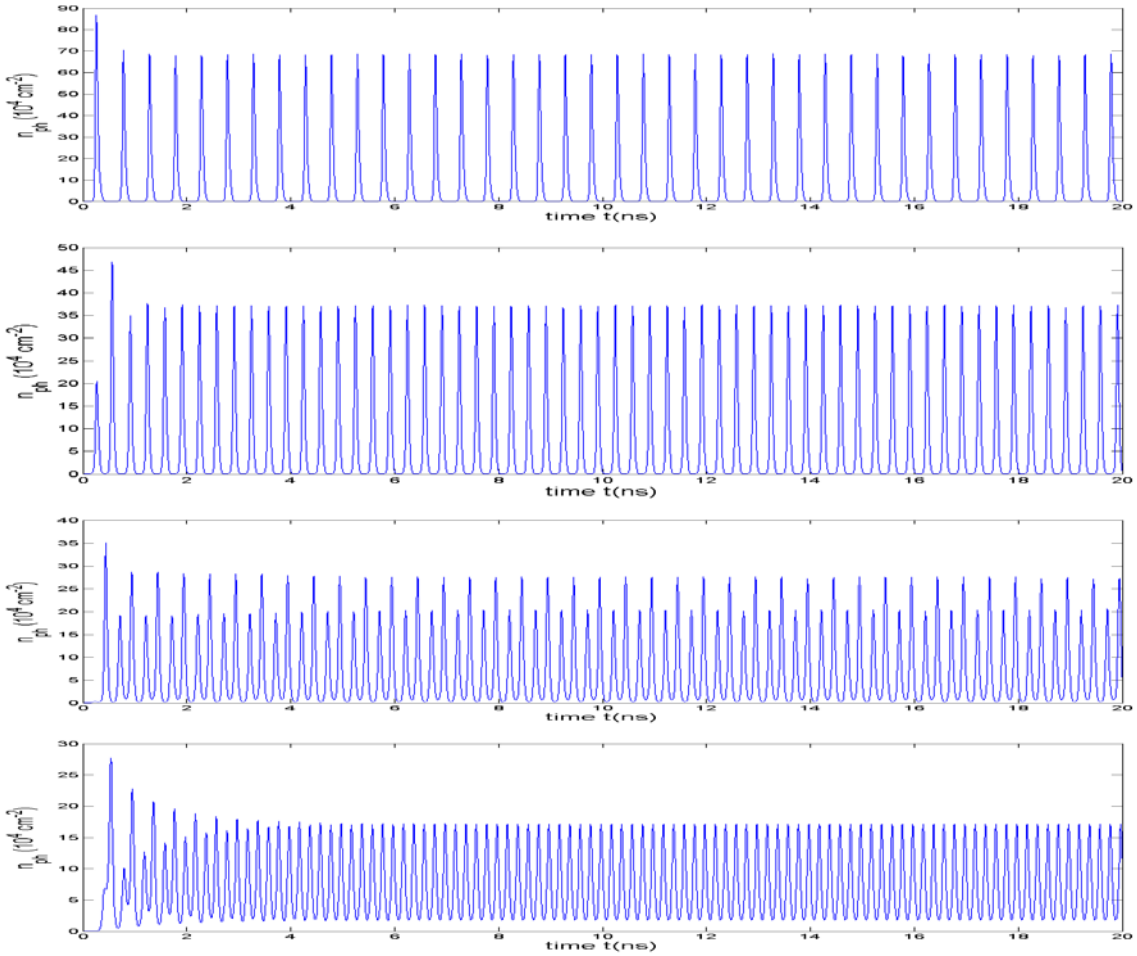

(i)

(ii)

(iii)

(iv)

Fig (13):Time series of photon density (n_{ph}) for selected bias strength, *b*, modulation depth ,*m*, and modulation frequency (GHz) , f_m ,(b,m, f_m): (i) 2.5, 9, 2 ;(ii) 2.5, 9 ,3;(iii)2.5,9,4; (iv) 2.5,9,5.

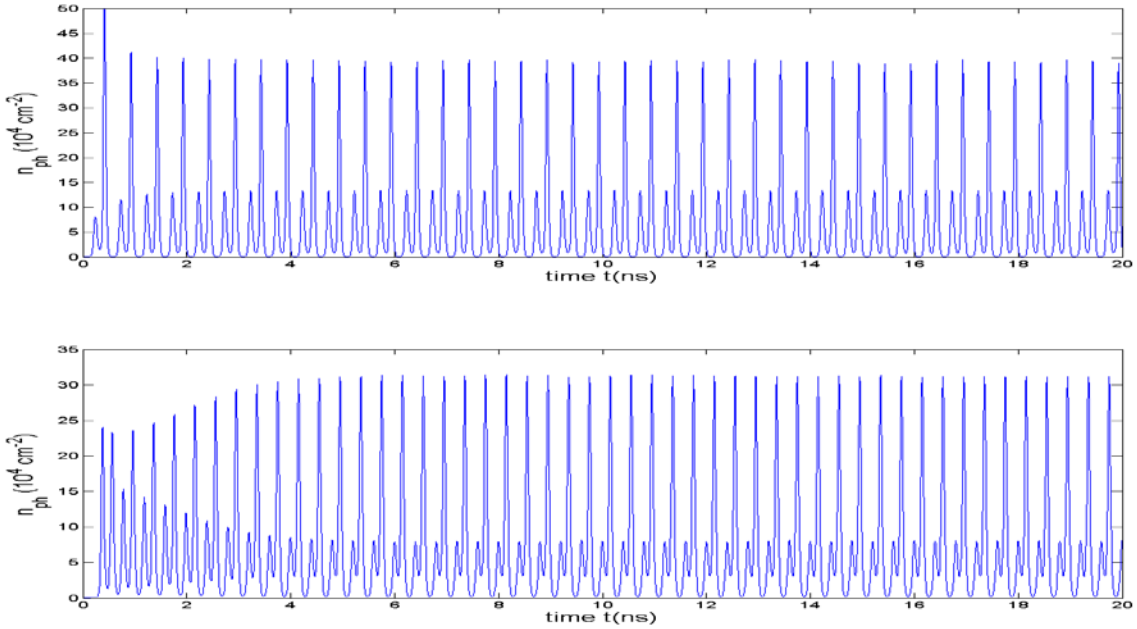

(i)

(ii)

Fig (14):Time series of photon density (n_{ph}) for selected bias strength, *b*, modulation depth ,*m*, and modulation frequency (GHz) , f_m ,(b,m, f_m): (i) 2.5, 14, 4 ;(ii) 2.5, 14 , 5 .

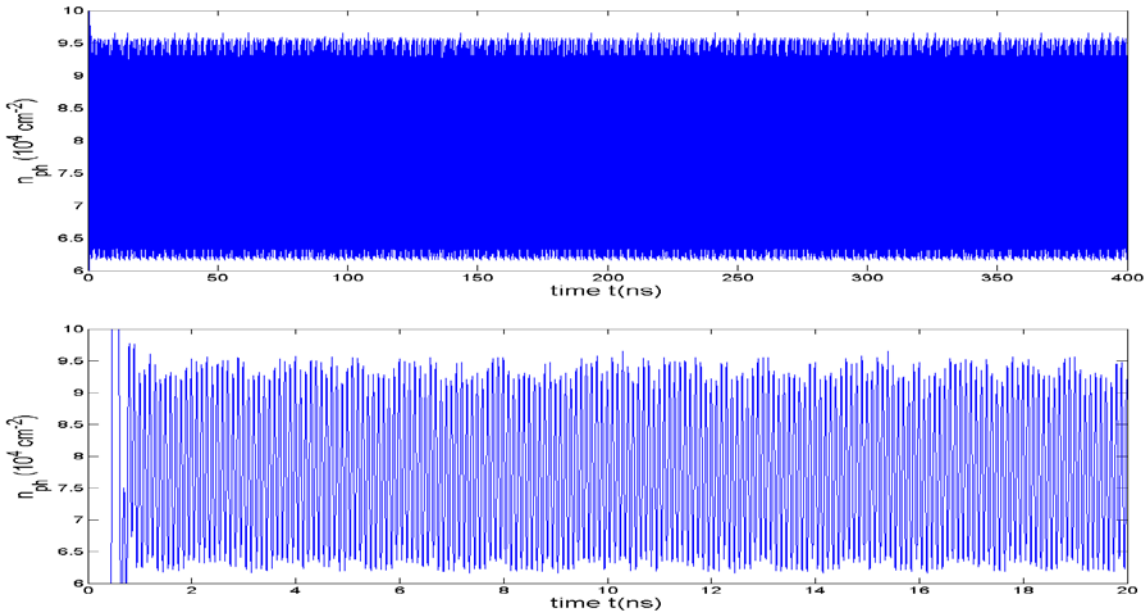

(i)

(ii)

Fig (15):Time series of photon density (n_{ph}) for selected bias strength, *b*, modulation depth ,*m*, and modulation frequency (GHz) , f_m ,(b,m, f_m): 2.5, 14 , 10 for two time bases :i (0-400 ns), ii (0-20 ns)

Conclusion:

We have investigated the effect of the modulating the injection current on the photon density of InAs/InGaAs quantum dot laser via the variation of the dc and ac parts of the injection current and the frequency of modulation. Bifurcation route to chaos appear to be the route that QDLs can take to reach chaos .Windows such as period 3 and intermittency seem to occur in this laser too. Output death phenomena seem to occur. Such effect was noticed in semiconductor lasers under the effect of feedback.

References

1-P.Harrison ,Quantum wells ,wires and dots , J. Wiley and sons, Sussex ,England (2005).

2- "Nonlinear laser dynamics ", Ed .K . Ludge ,Wiley –VCH Verlag GmBH and Co. KGaA ,Germany (2012) .

3-S.Rajesh,Nonlinear dynamics of semiconductor lasers :Control and synchronization of chaos ibid (2005).

4-P.U.Jijo,Nonlinear dynamics of multiple quantum well lasers: Chaos and multistability ,Cochin university of science and Technology ,India .Na(2005).

5-B.M.Krishna ,M.P.John and V.M. Nandakumaran ,Bidirectional communication using delay coupled chaotic directly modulated semiconductor lasers ,Pramana-j.phys.,74,177-188(2010) .

6-J.Ohtsubo ,Semiconductor lasers ,Stability ,Instability and chaos ,Springer series in optical sciences ,Springer –Verlag Berlin Hidelberg,(2008).

7- S.Rajesh and V.M. Nandakumaran , Control of bistability in a direct modulated Semiconductor laser using delay optoelectronic feedback , Physica D, 213,113-120,(2006) .

8-P.N.Melenetiev,M.V.Subbotin,and V.I.Balykin, Simple and effective

modulation of diode lasers ,Laser Phys. ,11,891-896(2001).
9- H .Saito, K .Nish, A .Kamei and S.Sugou,IEEE Phot.Tech.Lett.,12,1298-1300(2000).
10-K. Lüdge and E. Schöll, "Quantum-dot lasers—desynchronized nonlinear dynamics of electrons and holes," *IEEE J.QE*, 45, 1396– 1403,Nov.(2009).
11-C.Otto, K.Ludge and E.Scholl ,Modeling quantum dot lasers with optical feedback :sensitivity of bifurcation scenarios , Phys.State.Sol.B,247,829-829(2010).
12-F.T.Arecchi,Instabilities and chaos in lasers :Introduction to hyperchaos , Synergetics and dynamic instabilities ,99th course of E.Fermi School (1988).
13-M.O.Oleiwi and C.A.Emshary ,Dynamical behavior of quantum-dot laser ,J.Thi-Qar Science ,Acc. Publication(2013).
14-S.H.Strogate,Death by delay ,Nature ,394(1998).
15-J.Zamora-Munt,C.Masoller and J. Garcia-Ojalvo ,Crowed synchrony and quorum sensing in delay –coupled lasers ,Phys.Rev.Lett.,105,264101-1(2010).
16-H.A.Sultan,K.A.AL-Temimi,A.R,Ahmed and C.A.Emshary, The output dynamics of mutually coupled semiconductor face to face laser systems under noise effect , J. Bas. Res.(sciences),39,13-27(2013).
[17]- Modeling of Dynamics of Quantum Dot Lasers and Amplifiers, Project B2 (Sfb 787 Nanophotonics, 2008-2011).
[18]-A.M.Chekheim, Study the dynamics of vertical-cavity surface –emitting semiconductor laser (VCSEL),MSc ,Basrah University (2012).

[19]- V . Bindu and V.M. Nandakumaran, Numerical studies on bi-directionally coupled directly modulated semiconductor lasers ,Phys.Lett, A 277 ,345-351(2000).

تأثيرات تضمين التيار المباشر على كثافة الفوتونات في ليزر شبه الموصل نوع النقطة الكمية InAs/InGaAs

مشتاق عبيد عليوي جاسب عبد الحسين مشاري

قسم الفيزياء /كلية التربية للعلوم الصرفة /جامعة البصرة / البصرة –العراق

الخلاصة :

نتجـت حركـيات مختلفـــــة في خرج لـيزر InAs/InGaAs امتدت من دورة واحدة ولغاية الفوضى بتأثير النقطة الكمية

تضمين تيار الحقن اعتمادا على أنموذج نظري. كما لوحظت ظاهرة موت الخرج في هذا الليزر . نتج من عمليتي التضمين الشديد والضعيف لتيار الحقن حالات فوضوية و بدا أن الوصول لحالة الفوضى يتبع مسار التفرع .